Supplementary Figure 1

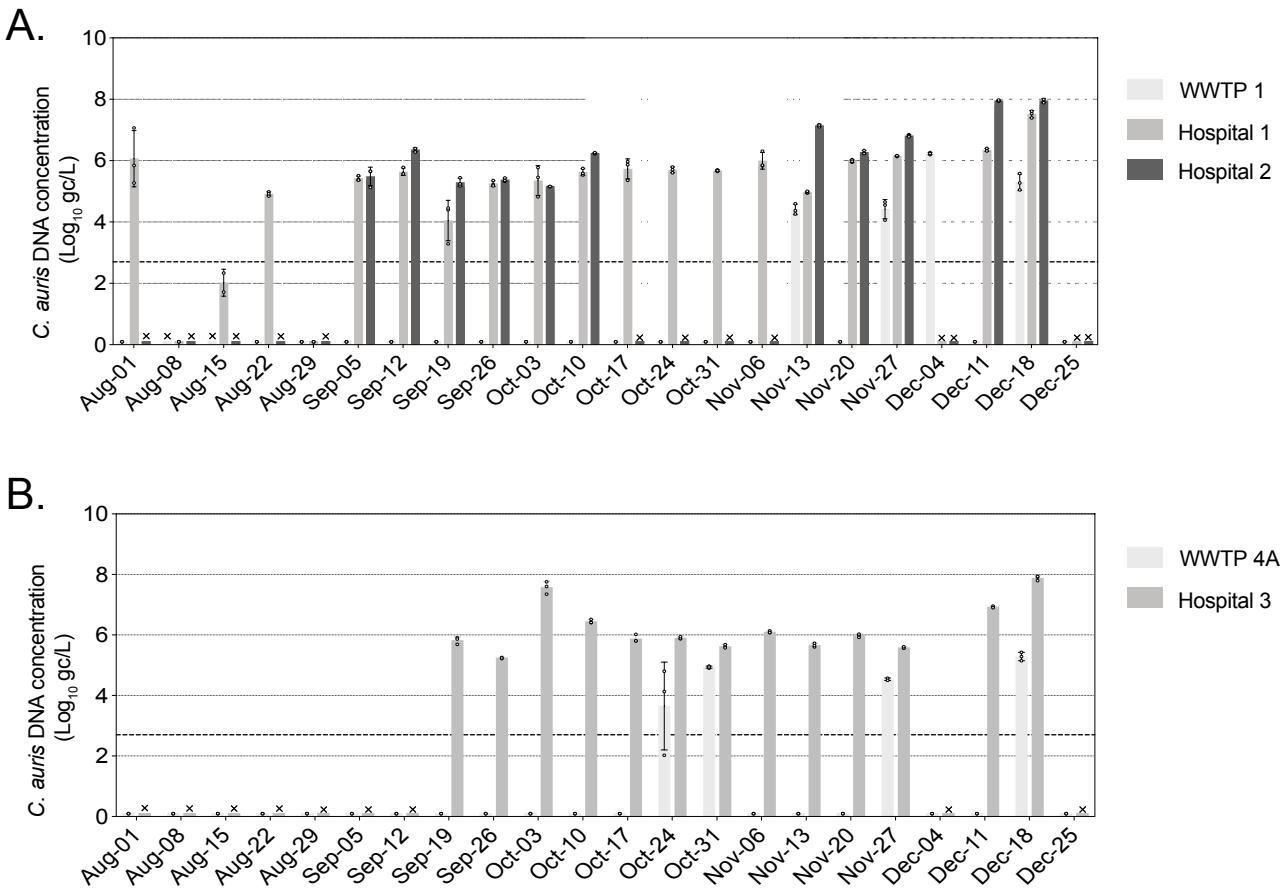

Supplementary Fig. 1. Enhanced sensitivity of facility-level wastewater surveillance for *C. auris* detection.
Weekly *C. auris* DNA concentrations (log_{10} gc/L) quantified by qPCR from August–December 2023. (A) Temporal distribution of concentrations for WWTP1, Hospital 1, and Hospital 2. (B) Temporal distribution of concentrations for WWTP4A and Hospital 3. Each data point represents an individual qPCR measurement plotted over time. The limit of quantification (LoQ) is 500 gc/L (corresponding to 2.70 log_{10} gc/L). Cross (X) marks indicate dates when no sample was collected. Hospital wastewater showed significantly higher detection frequency (95.4% vs. 18.4%; Fisher's exact test, odds ratio = 0.0109, $p < 0.001$) and significantly higher concentrations (two-sided Mann–Whitney U = 15,341.5, n = 130 hospital, 125 WWTP), demonstrating the dilution effect in municipal systems and the superior sensitivity of upstream facility-level surveillance for *C. auris* outbreak monitoring. Source data are included in the Source Data 8 file.

Supplementary Figure 2

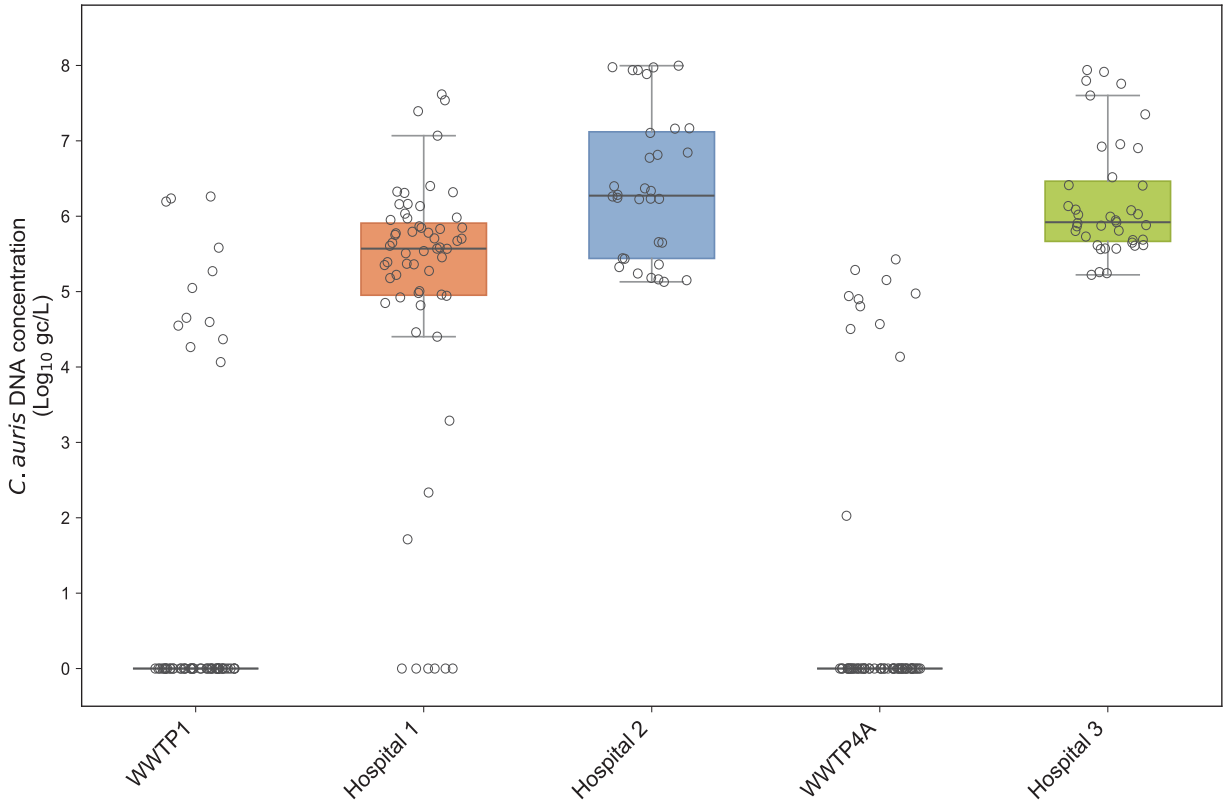

Supplementary Fig. 2. *C. auris* DNA concentrations are significantly higher in hospital wastewater than treatment plants. Box plot comparison of C. auris DNA concentrations (log_{10} gc/L) across five sampling locations during August-December 2023: WWTP1, Hospital 1 (orange), Hospital 2 (blue), WWTP4A, and Hospital 3 (green). Boxes show median and interquartile range (IQR), whiskers extend to 1.5× IQR, and circles represent individual replicates. Hospital wastewater samples exhibited significantly elevated concentrations and more consistent detection compared to WWTPs (Mann-Whitney U = 15,341.5, $p < 0.001$). Hospital 2 showed the highest and most consistent levels, while Hospitals 1 and 3 displayed broader concentration ranges. WWTPs showed sporadic low-level detections with most samples near or below detection limits, demonstrating nearly two orders of magnitude difference between maximum hospital and WWTP concentrations. Source data are included in the Source Data 8 file.

Supplementary Figure 3

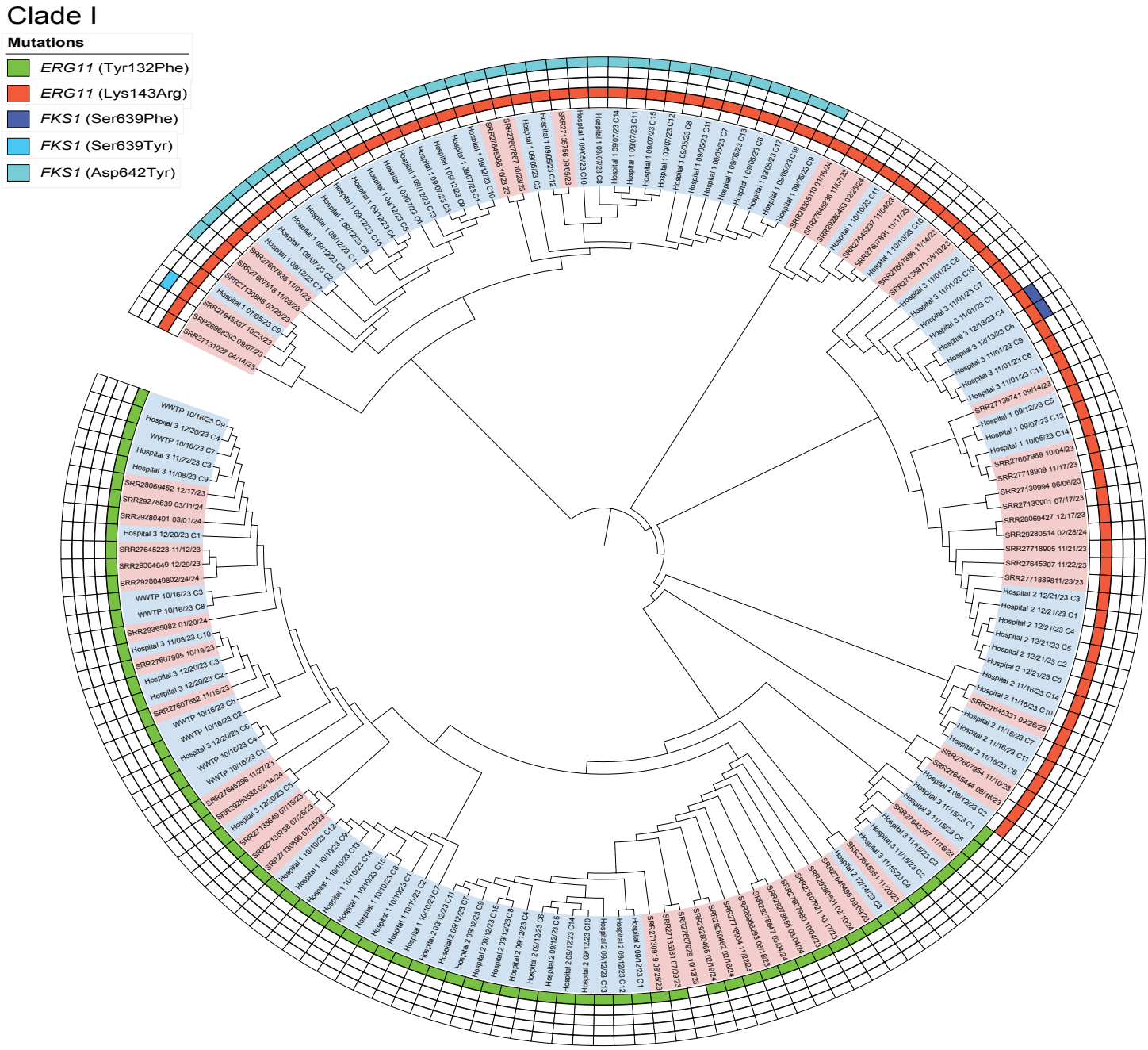

Supplementary Fig. 3. *C. auris* Clade I phylogeny reveals multiple subclades and high wastewater-clinical concordance. Maximum likelihood phylogenetic tree of Clade I *C. auris* isolates from Southern Nevada (August 2021-August 2024) based on core genome SNPs. Clinical isolates shown with pink label background, wastewater isolates with blue label background. Outer rings display resistance mutations color-coded by variant: *ERG11* Tyr132Phe (green), *ERG11* Lys143Arg (red), *FKS1* Ser639Phe (dark blue), *FKS1* Ser639Tyr (cyan), *FKS1* Asp642Tyr (teal). Wastewater isolate labels indicate facility, collection date (MM/DD/YY), and colony ID; clinical isolates are identified by SRA accession number and collection date. The tree reveals multiple subclades with distinct resistance patterns. *ERG11* Tyr132Phe mutations (azole resistance) cluster in specific phylogenetic groups, while *FKS1* mutations (echinocandin resistance) show scattered distribution. High genomic concordance is evident, with >90% of wastewater isolates clustering within 0-3 SNPs of clinical sequences. This close genetic relationship demonstrates that wastewater surveillance captures active pathogen transmission from colonized or infected individuals rather than distinct environmental populations, validating wastewater monitoring as a reliable indicator of clinical outbreak dynamics. Source data are included in the Source Data 9 file.

Supplementary Figure 4

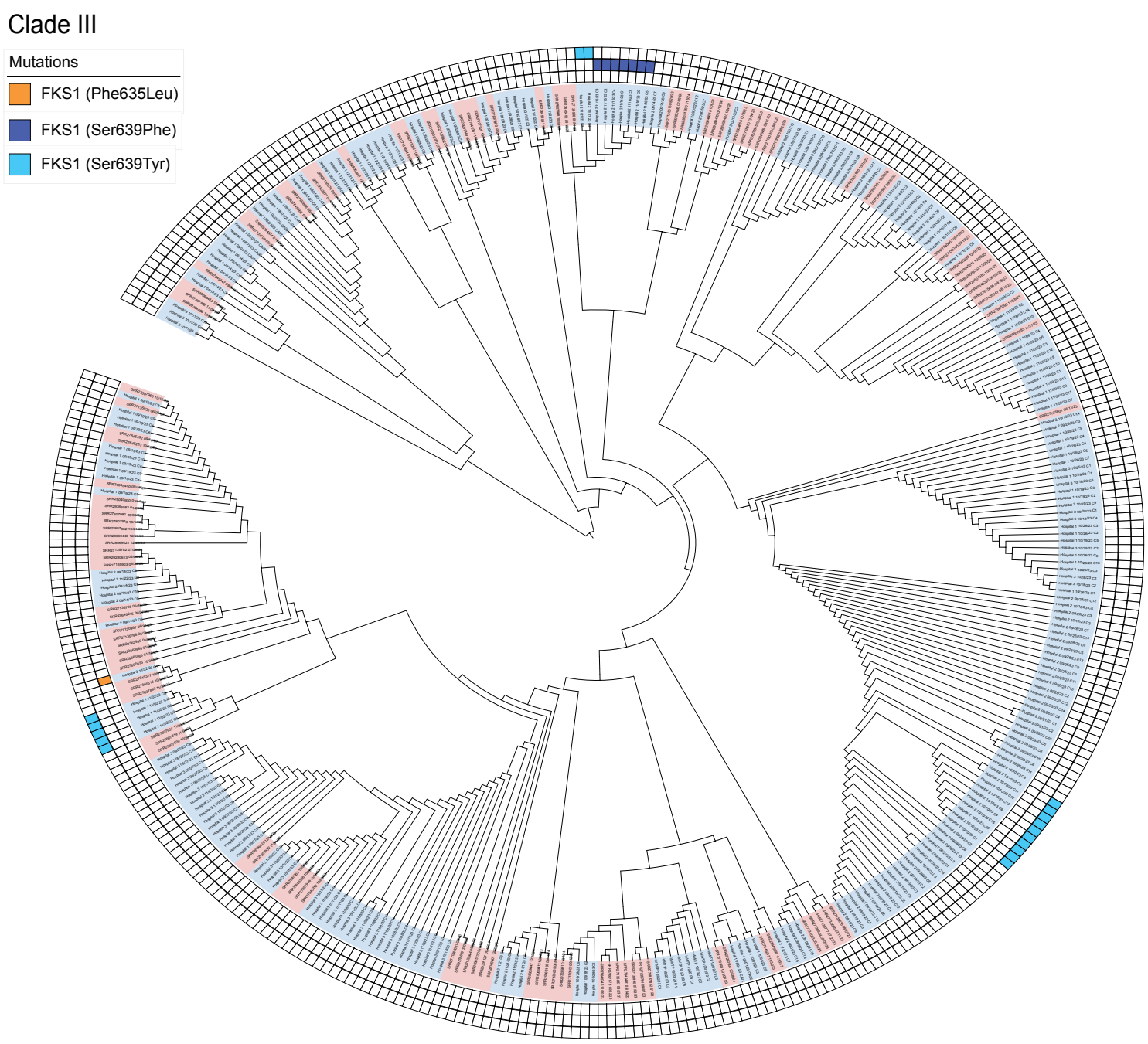

Supplementary Fig. 4. *C. auris* Clade III phylogeny reveals distinct subclades harboring FKS1 resistance mutations. Maximum likelihood phylogenetic tree of Clade III *C. auris* isolates from Southern Nevada (August 2021–August 2024) based on core genome SNPs. Clinical isolates shown with pink label background, wastewater isolates with blue label background. Outer rings display *FKS1* mutations associated with echinocandin resistance, color-coded by variant: Phe635Leu (orange), Ser639Phe (dark blue), Ser639Tyr (cyan). Wastewater isolate labels indicate facility, collection date (MM/DD/YY), and isolate ID; clinical isolates are identified by SRA accession number and collection date. The tree reveals multiple subclades with distinct temporal and spatial distributions. *FKS1* mutations show markedly higher prevalence in wastewater isolates (16.2%) compared to clinical isolates (2.2%). The phylogeny demonstrates facility-specific clustering patterns and reveals several previously unreported subclades, including rare *FKS1* Phe635Leu mutations that were first detected in wastewater prior to their identification in clinical isolates. Close phylogenetic relationships between wastewater and clinical isolates (>90% concordance within 3 SNPs) support wastewater surveillance as an effective early warning system for tracking emerging resistance patterns before widespread clinical detection. Source data are included in the Source Data 10 file.

Supplementary Figure 5

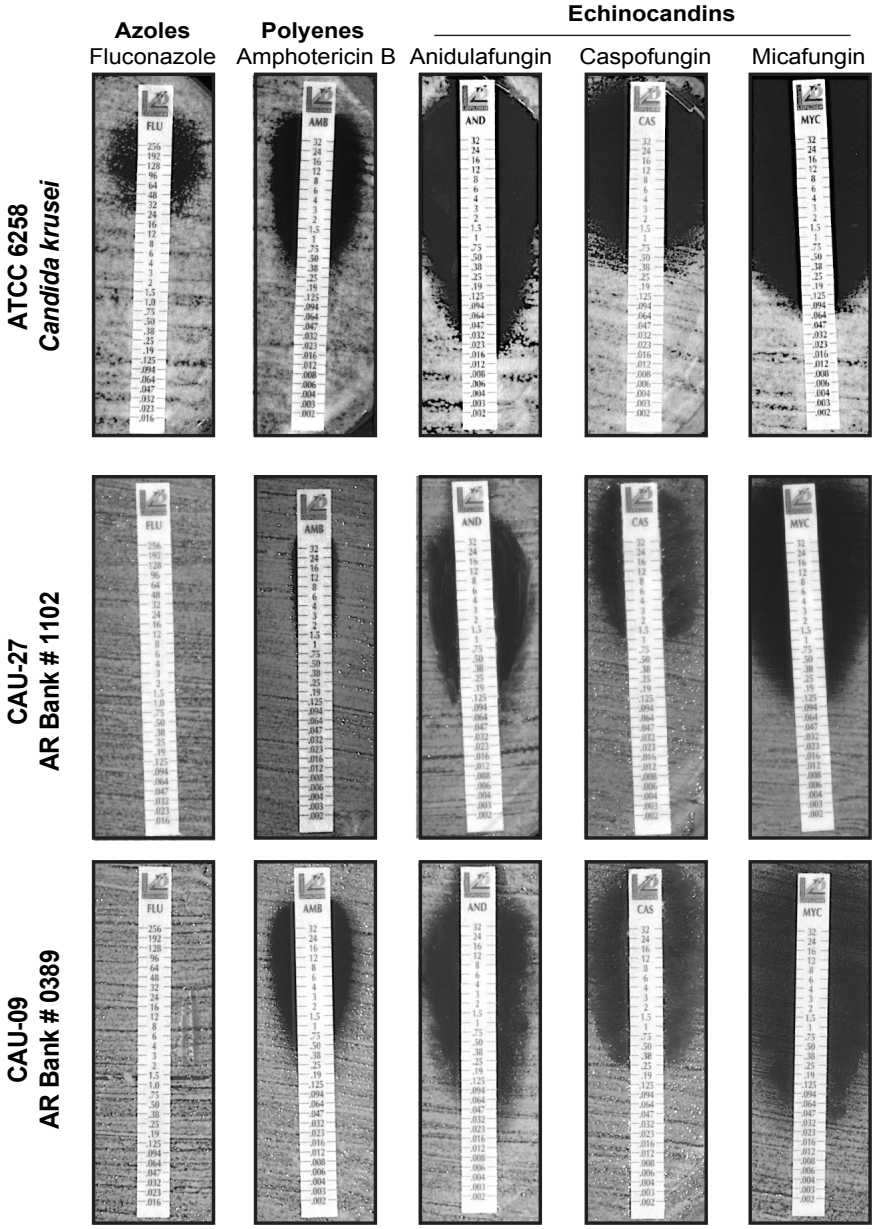

Supplementary Fig. 5. Quality control strains validate antifungal susceptibility testing performance.

Gradient diffusion MIC strips for quality control strains across five antifungals in three drug classes, performed in biological triplicate. Top: ATCC 6258 (*C. krusei)*. Middle: CAU-27/AR-1102 (*C. auris* Clade III). Bottom: CAU-09/AR-0389 (*C. auris* Clade I). Columns show Azoles (Fluconazole), Polyenes (Amphotericin B), and Echinocandins (Anidulafungin, Caspofungin, Micafungin). Elliptical inhibition zones intersect gradient strips at MIC values. All strains yielded MIC values within established reference ranges, validating assay performance for wastewater-derived and clinical isolate susceptibility testing in the study.

Supplementary table 1

Gene	Accession	Position: Start	Position: End
CDR1	PEKT02000001.1	348521	353047
C. albicans unique	NC_032089.1	66764	67698
C. auris unique	PEKT02000007.1	172646	173634
ERG11	PEKT02000003.1	832733	834307
ERG3	PEKT02000007.1	2369962	2371053
ERG6	PEKT02000010.1	960572	961699
FKS1	PEKT02000002.1	1002873	1008539
HSP90	PEKT02000010.1	61761	63887
MEC3	PEKT02000007.1	1041428	1042390
MLH1	PEKT02000008.1	783713	785689
MRR1A	PEKT02000007.1	3093802	3096522
TAC1B	PEKT02000009.1	814591	817197
UPC2	PEKT02000001.1	559186	561039

Supplementary Table 1. Genomic coordinates of amplicon panel targeting *C. auris* resistance-associated genes. Custom amplicon panel designed to detect antifungal resistance mutations in *C. auris* wastewater samples. The panel targets 11 genes implicated in resistance mechanisms: *CDR1, ERG3, ERG6, ERG11, FKS1, HSP90, MEC3, MLH1, MRR1A, TAC1B*, and *UPC2*. Additional species-specific markers for *C. auris* and *C. albicans* were included to enable species discrimination in complex wastewater matrices. Genomic positions are based on the *C. auris* strain B8441 V2 reference genome (GCA_002759435.2). Gene accession numbers and start/end positions are provided for each target.

Supplementary table 2.

SNP distance to closest clinical isolate	Number of wastewater isolates	Percentage
0	50	47.6%
1	28	26.7%
2	10	9.5%
3	7	6.7%
4+	8	7.6%
none	2	1.9%
total	105	100.0%

Supplementary Table 2. Genomic concordance between wastewater and clinical *C. auris* isolates.

SNP distance analysis showing genetic similarity between 105 unique wastewater isolates and their closest clinical matches. SNP distances were calculated to the nearest clinical isolate for each wastewater genome. Nearly half (47.6%) of wastewater isolates showed exact matches (0 SNPs) to clinical isolates, and 90% were within 3 SNPs of clinical sequences, demonstrating high genomic concordance. Only two wastewater isolates (1.9%) had no close clinical matches, representing potentially unique environmental lineages or pre-clinical detection of emerging subclades. This high degree of genetic similarity supports the interpretation that wastewater surveillance captures active pathogen transmission from colonized or infected individuals rather than distinct environmental populations.